

Course 12.812, General Circulation of the Earth's Atmosphere
 Prof. Peter Stone
Section 6: Spectral Analysis

Fourier Analysis is particularly well adapted for giving information about the scale dependences in any field, something that is not readily extracted from the diagnostics that we have looked at previously. The fields can be Fourier analyzed with respect to t , x , y , or z and information extracted about the corresponding scales. Most of the analyses that have been carried out have been concerned with the longitudinal variations, and this is what we will concentrate on. (In recent years some work has also been done on analysis of the t and y spectra.)

Let $\lambda = \text{longitude}$, $0 \leq \lambda < 2\pi$. Then any real bounded field, f , can be represented by a Fourier series, with $n = \text{zonal wave number}$:

$$f(\lambda) = A_0 + \sum_{n=1}^{\infty} A_n \cos n\lambda + \sum_{n=1}^{\infty} B_n \sin n\lambda,$$

$$\text{where } A_0 = \frac{1}{2\pi} \int_0^{2\pi} f d\lambda, \quad A_n = \frac{1}{\pi} \int_0^{2\pi} f \cos n\lambda d\lambda, \quad \text{and } B_n = \frac{1}{\pi} \int_0^{2\pi} f \sin n\lambda d\lambda.$$

It is convenient to put this representation in a complex form analogous to a Fourier Transform pair. If we substitute

$$\cos n\lambda = \frac{1}{2}(e^{in\lambda} + e^{-in\lambda}), \quad \sin n\lambda = \frac{1}{2i}(e^{in\lambda} - e^{-in\lambda}),$$

$$\text{then } f(\lambda) = A_0 + \sum_{n=1}^{\infty} \left\{ \frac{1}{2}(A_n - iB_n)e^{in\lambda} + \frac{1}{2}(A_n + iB_n)e^{-in\lambda} \right\};$$

The second summation can be written as

$$\sum_{n=1}^{\infty} \frac{1}{2}(A_n + iB_n)e^{-in\lambda} = \sum_{m=-1}^{-\infty} \frac{1}{2}(A_{-m} + iB_{-m})e^{im\lambda}.$$

\therefore we can write $f(\lambda)$ as a single summation,

$$f(\lambda) = \sum_{n=-\infty}^{\infty} \tilde{f}(n) e^{in\lambda}, \quad \text{where } \tilde{f}(n) \text{ is a generalized Fourier coefficient,}$$

$$\tilde{f}(n) = \begin{cases} \frac{1}{2}(A_n - iB_n), & n \geq 1 \\ A_0, & n = 0 \\ \frac{1}{2}(A_{-n} + iB_{-n}), & n \leq -1 \end{cases}, \quad \text{N.B., } \tilde{f}(-n) = \tilde{f}^*(n),$$

where the asterisk here denotes the complex conjugate.

This can be written in more compact form:

$$\text{For } n \geq 1, \tilde{f} = \frac{1}{2\pi} \int_0^{2\pi} f \cos n\lambda d\lambda - \frac{i}{2\pi} \int_0^{2\pi} f \sin n\lambda d\lambda = \frac{1}{2\pi} \int_0^{2\pi} f e^{-in\lambda} d\lambda$$

$$\text{For } n = 0, \tilde{f} = \frac{1}{2\pi} \int_0^{2\pi} f d\lambda = \frac{1}{2\pi} \int_0^{2\pi} f e^{-in\lambda} d\lambda,$$

$$\text{For } n \leq -1, \tilde{f} = \frac{1}{2\pi} \int_0^{2\pi} f \cos(-n\lambda) d\lambda + \frac{i}{2\pi} \int_0^{2\pi} f \sin(-n\lambda) d\lambda = \frac{1}{2\pi} \int_0^{2\pi} f e^{-in\lambda} d\lambda.$$

$$\therefore f(\lambda) = \sum_{n=-\infty}^{\infty} \tilde{f}(n) e^{in\lambda}, \quad \tilde{f}(n) = \frac{1}{2\pi} \int_0^{2\pi} f e^{-in\lambda} d\lambda$$

relates any real field $f(\lambda)$ to its spectral representation $\tilde{f}(n)$.

Example: One drive for stationary eddies is longitudinal variations of condensation resulting from longitudinal variations of evaporation. For example, in winter, when the oceans are warmer than the land, one expects the oceans to be a much larger source of evaporation and condensation than the land. Suppose we assume uniform but different rates for evaporation and condensation over land and over ocean. What is the spectrum of this latent heating function, Q , -- i.e., what spectrum would we expect stationary eddies driven by this mechanism to have? Suppose we calculate the spectrum at 38N. At this latitude, the width of the oceans and continents is shown in the first line below.

	Pacific	North America	Atlantic	Eurasia
Observed	120°	45°	65°	130°
Approximation	120°	60°	60°	120°

In order to simplify our calculation we will make the approximation indicated. Then the distribution of $Q^* = Q - [Q]$ is as shown below.

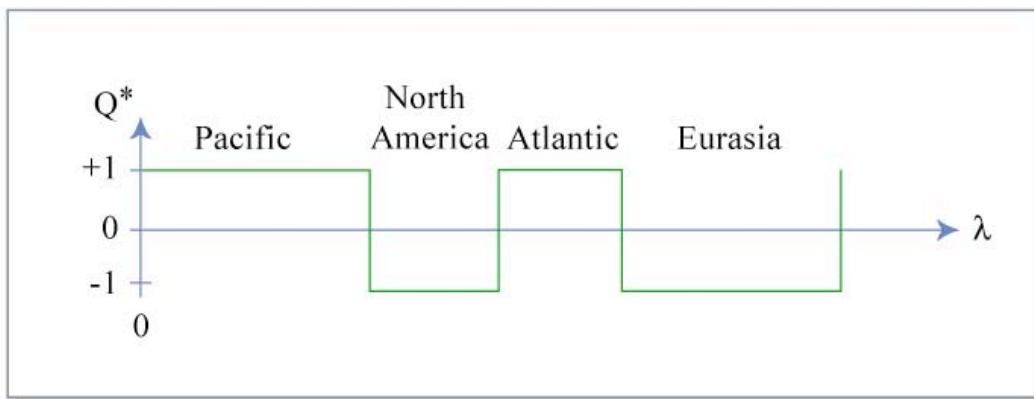


Figure by MIT OCW.

(Note that the amplitude is arbitrary since we are interested in the spectral distribution.)

$$\begin{aligned} \therefore \tilde{Q}^* &= \frac{1}{2\pi} \int_0^{2\pi} Q^* e^{-in\lambda} d\lambda = \frac{1}{2\pi} \left[\int_0^{2\pi/3} e^{-in\lambda} d\lambda - \int_{2\pi/3}^{\pi} e^{-in\lambda} d\lambda + \int_{\pi}^{4\pi/3} e^{-in\lambda} d\lambda - \int_{4\pi/3}^{2\pi} e^{-in\lambda} d\lambda \right] \\ &= \frac{i}{\pi n} \left[e^{-in\frac{2\pi}{3}} + e^{-in\frac{4\pi}{3}} - 1 - (-1)^n \right]; \end{aligned}$$

The quantity in brackets is a symmetric cyclic function of u with period $n = 6$, and each successive cycle decays $\sim \frac{1}{n}$. In particular, $\tilde{Q}^* = \frac{i}{\pi n} [-1, -3, 2, -3, -1, 0, \dots]$.

Also we recall that $\tilde{Q}^* = \frac{1}{2}(A_n - iB_n)$; $n > 0$

and $A_n = 0$, and the only non-trivial components, for our choice of phase, are the sine components;

$$\therefore B_n = \frac{2}{\pi n} [1, 3, -2, 3, 1, 0, \dots].$$

The magnitude of the first twelve components are tabulated below, and plotted.

n	1	2	3	4	5	6	7	8	9	10	11	12
$\frac{\pi}{2} B_n $ or $\pi \tilde{Q}^* $	1	1.5	.67	.75	.2	0	.14	.38	.22	.3	.09	0

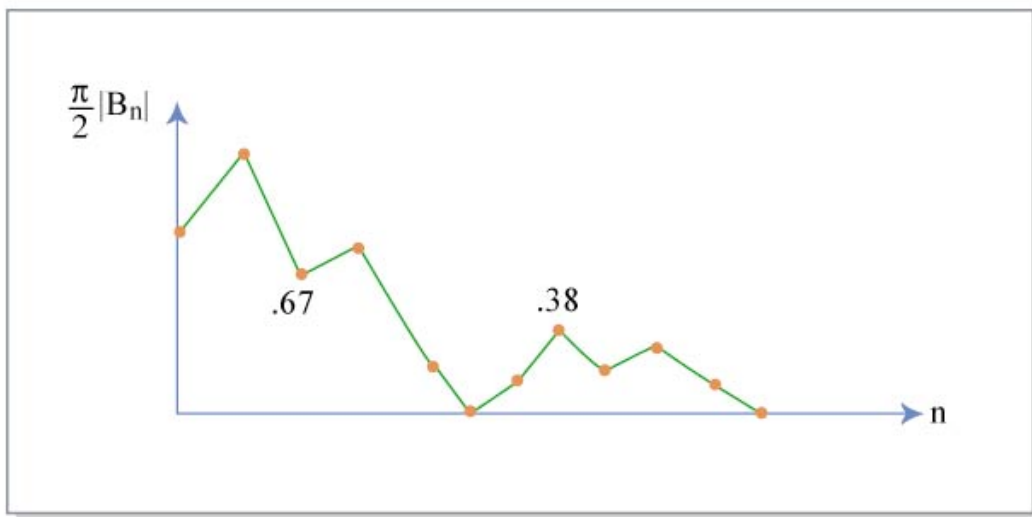


Figure by MIT OCW.

We see that most of the signal is in the first 4 wave numbers with the peak at wave number 2. This spectrum is typical of the distribution of continents in Northern mid-latitudes, and is also typical of the spectrum of forcing due to topographic effects, since mountains are highly correlated with continents.

Spectra of zonal mean quadratic terms:

Spectral analyses of various quadratic terms are also of particular interest – e.g., what scales dominate in transporting heat poleward? These quantities generally involve cross-correlations, and to illustrate their spectral analyses we will analyze the spectrum of $[v'T']$. Let

$H = [v'T'] = \sum_{n=0}^{\infty} H_n$, where H_n represents the contribution to H by scales with wave numbers $\pm n$. Our problem is to relate H_n to $\tilde{v}'(n)$ and $\tilde{T}'(n)$.

We start this time from the generalized Fourier Form:

$$v' = \sum_{n=-\infty}^{\infty} \tilde{v}'(n) e^{in\lambda}, T' = \sum_{n=-\infty}^{\infty} \tilde{T}'(n) e^{in\lambda},$$

In T' , let $n = -m$;

$$\therefore T' = \sum_{m=-\infty}^{+\infty} \tilde{T}'(-m) e^{-im\lambda};$$

$$\therefore v'T' = \sum_{n=-\infty}^{\infty} \sum_{m=-\infty}^{\infty} \tilde{v}'(n) \tilde{T}'(-m) e^{i(n-m)\lambda};$$

$$\therefore [v'T'] = \sum_{n,m} \tilde{v}'(n) \tilde{T}'(-m) \frac{1}{2\pi} \int_0^{2\pi} e^{i(n-m)\lambda} d\lambda = \sum_{n=-\infty}^{\infty} \tilde{v}'(n) \tilde{T}'(-n), \text{ since}$$

$$\frac{1}{2\pi} \int_0^{2\pi} e^{i(n-m)\lambda} d\lambda = \begin{cases} 0, & \text{if } n \neq m \\ 1, & \text{if } n = m \end{cases}$$

$$\therefore [v'T'] = \tilde{v}'(0)\tilde{T}'(0) + \sum_{n=1}^{\infty} \tilde{v}'(n)\tilde{T}'(-n) + \sum_{n=-\infty}^{-1} \tilde{v}'(n)\tilde{T}'(-n);$$

Now let $n = -m$ in the second sum, and it becomes $\sum_{m=1}^{\infty} \tilde{v}'(-m)\tilde{T}'(m)$, \therefore we can combine

to write

$$[v'T'] = \tilde{v}'(0)\tilde{T}'(0) + \sum_{n=1}^{\infty} \{ \tilde{v}'(n)\tilde{T}'(-n) + \tilde{v}'(-n)\tilde{T}'(n) \}$$

The $n = 0$ term we identify as the transport associated with time variations in the MMC. In Oort & Peixoto's definition this is included in the TE transport, although in many studies it is not. Also, now we can identify

$$H_n = \tilde{v}'(n)\tilde{T}'(-n) + \tilde{v}'(-n)\tilde{T}'(n) \text{ for } n \geq 1.$$

This gives the spectrum for the sensible heat transport.

It is easy to generalize this result for any quadratic quantity. E.g., if

$$M = [v'u'] = \sum_{n=0}^{\infty} M_n, \text{ then } M_n = \tilde{v}'(n)\tilde{u}'(-n) + \tilde{v}'(-n)\tilde{u}'(n) \text{ for } n \geq 1. \quad M_0 = \tilde{v}'(0)\tilde{u}'(0)$$

$$\text{Another example: zonal mean kinetic energy, } [K] = \frac{1}{2}[u^2 + v^2] = \sum_{n=0}^{\infty} K_n;$$

$$\therefore K_0 = \text{mean K.E.} = \frac{1}{2}\{\tilde{u}^2(0) + \tilde{v}^2(0)\}; \text{ and}$$

$$K_n = \frac{1}{2}\{\tilde{u}(n)\tilde{u}(-n) + \tilde{u}(-n)\tilde{u}(n) + \tilde{v}(n)\tilde{v}(-n) + \tilde{v}(-n)\tilde{v}(n)\};$$

$$\therefore K_n = \tilde{u}(n)\tilde{u}(-n) + \tilde{v}(n)\tilde{v}(-n);$$

$$\text{And we recall } \tilde{u}(-n) = \tilde{u}^*(n), \text{ etc., } \therefore K_n = \tilde{u}(n)\tilde{u}^*(n) + \tilde{v}(n)\tilde{v}^*(n), \quad n \geq 1$$

Example: consider the heat transport by the simple v, T fields

$$v' = v_0(t) \begin{cases} +1, & -\lambda_0 < \lambda < 0 \\ -1, & 0 < \lambda < \lambda_0 \\ 0, & \text{elsewhere} \end{cases}$$

$$T' = T_0(t) \begin{cases} +1, & -\lambda_0 < \lambda < 0 \\ -1, & 0 < \lambda < \lambda_0 \\ 0, & \text{elsewhere} \end{cases}$$

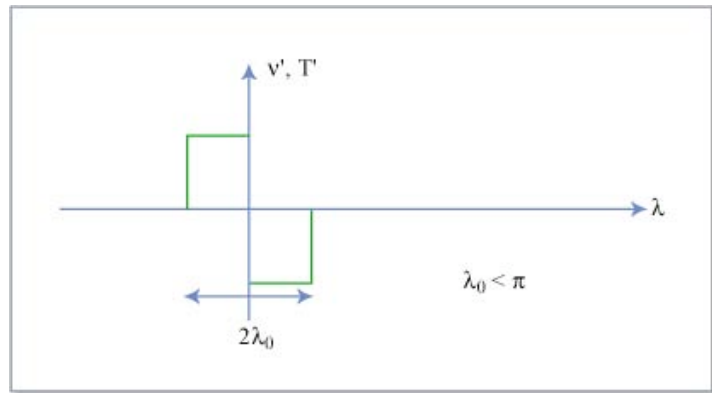


Figure by MIT OCW.

This can be thought of as a simple representation of a localized baroclinic cyclone, with the v and T anomalies in perfect phase.

$$\begin{aligned}\tilde{v}(n) &= \frac{1}{2\pi} \int_0^{2\pi} v(\lambda) e^{-in\lambda} d\lambda = \frac{v_0}{2\pi} \left\{ \int_{-\lambda_0}^0 e^{-in\lambda} d\lambda - \int_0^{\lambda_0} e^{-in\lambda} d\lambda \right\} \\ &= -\frac{v_0}{2\pi in} \{1 - e^{in\lambda_0} - e^{-in\lambda_0} + 1\} = -\frac{v_0}{i\pi n} (1 - \cos n\lambda_0) \\ &= \frac{2v_0}{\pi in} \sin^2 \frac{n\lambda_0}{2}.\end{aligned}$$

Similarly, $\tilde{T}(n) = \frac{2T_0}{\pi in} \sin^2 \frac{n\lambda_0}{2}$.

$$\therefore H_n = \tilde{v}(n)\tilde{T}(-n) + \tilde{v}(-n)\tilde{T}(n) = \frac{8v_0T_0}{\pi^2 n^2} \sin^4 \frac{n\lambda_0}{2}.$$

If $\lambda_0 \ll 1$, at $n = 1$, $\text{amp} \sim \left(\frac{\lambda_0}{2}\right)^4$; at $n = \frac{\pi}{\lambda_0}$, $\text{amp} \sim \frac{1}{n^2} = \frac{\lambda_0^2}{\pi^2}$. The first is smaller if

$$\lambda_0^2 < \frac{16}{\pi^2}, \lambda_0 < \frac{4}{\pi}; \therefore 2\lambda_0 < \frac{8}{\pi} = 146^\circ.$$

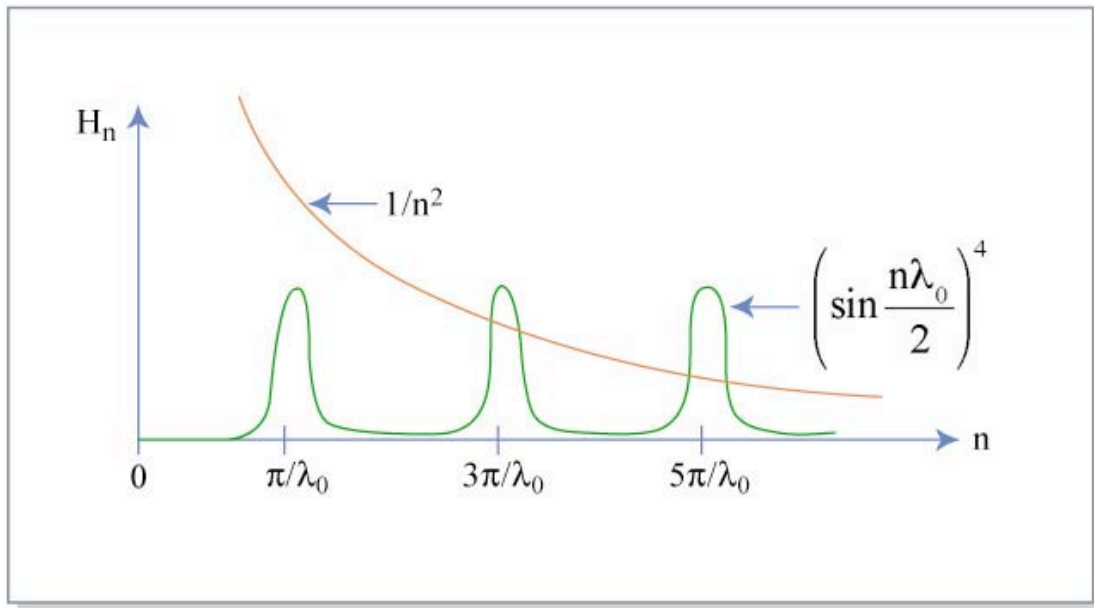


Figure by MIT OCW.

\therefore The peak is at $n = \frac{\pi}{\lambda_0}$ and this is large if λ_0 is small, with a

$$\text{wave-length} = \frac{2\pi}{\pi/\lambda_0} = 2\lambda_0 = \text{width of cyclone}.$$

Observations of K_n : The most complete analysis done to date of K_n is that of Winn-Nielson (1967). The basic procedure is to take analyzed fields of u and v and calculate their transforms by numerical integration, i.e., $\tilde{u}(n) = \frac{1}{2\pi} \int_0^{2\pi} u(p, \phi, t) e^{-in\lambda} d\lambda$, etc., are evaluated numerically for $n = 1, 2, \dots, N$ at any given time, latitude, latitude, and pressure level.

The value of N chosen depends on the longitudinal resolution of the data – for the normal observational network in the Northern Hemisphere in mid-latitudes, resolution limits one to $N \lesssim 15$. Then one calculates K_n from the Fourier Transforms for each n . Finally, if desired, the values of K_n at each t, ϕ, p can be integrated over t, ϕ, p .

Winn-Nielson calculated K_n for each day during the year. Feb. 1963 – Jan. 1964, inclusive, at 8 pressure levels (1000, 850, 700, 500, 300, 200, 150, and 100mb). He used NMC analyses which extended from 22N to the pole. Thus the resulting K_n is essentially an annual average over the troposphere for mid and high latitudes. The spectrum is shown in Fig. 21 of Winn-Nielson (1967). It is relatively flat, for $n \lesssim 6$, and then falls off steeply, with a nearly linear relation in logarithmic coordinates for $n \geq 8$. A least squares fit for $8 \leq n \leq 15$ gave the result $K_n \sim n^{-2.83}$.

This is particularly interesting, because it can be compared with predictions of turbulence theories that predict what the slope of $\log K_n$ vs $\log n$ should be in wave-number ranges where no energy is being generated or dissipated. (The energy generation occurs primarily for $n < 8$, due to topographic and baroclinic processes, and the dissipation primarily for $n \gg 15$.) In 3-D turbulence the slope should be $-5/3$, and in 2-D or quasi-geostrophic turbulence it should be -3 . In fact the atmosphere appears to fall in this second regime.

Turbulence Theories:

Consider homogeneous, isotropic, 3D stationary turbulence. Assume that there is an inertial subrange, in which no energy is generated or dissipated. Then energy is conserved in this range, and must cascade from the wave numbers, where it is generated (presumably small wave numbers) to those where it is dissipated (by viscosity, i.e., a large wave number). The cascade rate (generation rate = dissipation rate) is

$$\epsilon = \frac{dK}{dt} = \text{constant, where } K = \text{energy density} = \frac{1}{2} \vec{v} \cdot \vec{v}.$$

$\therefore \epsilon$ has dimensions $L^2 T^{-3}$;

The energy spectrum of K_n for an isotropic situation is only dependent on the total wave number, $\vec{n} \cdot \vec{n} = n^2$, and we can write $K = \int_0^\infty K_n dn$ (analogous to our \sum_n for our discrete spectra, i.e. $\sum_{n=0}^\infty K_n \rightarrow \int_0^\infty K(n)dn$, but the n 's are different, this one has dimensions).

$\therefore K_n$ has the dimensions L^3T^{-2} .

According to the Kolmogorov hypothesis, K_n will depend only on ϵ and n (the localness hypothesis). \therefore dimensional arguments require:

$$K_n = f(\epsilon, n) = \alpha \epsilon^j n^k;$$

$$\therefore L^3T^{-2} = (L^2T^{-3})^j L^{-k}$$

$$\therefore 2j - k = 3; \quad -2 = -3j$$

$$\therefore j = \frac{2}{3}; \quad k = \frac{4}{3} - 3 = -\frac{5}{3}$$

$$\therefore K_n = \alpha \epsilon^{2/3} n^{-5/3}$$

This result has been verified for 3D turbulence, and experiments yield $\alpha \cong 1.5$.

However, the situation in 2D turbulence is different. Now both energy and enstrophy, P , are conserved,

$$P = \frac{1}{2} \nabla \times \vec{v} \cdot \nabla \times \vec{v}.$$

\therefore there are two distinct possibilities: an inertial subrange controlled by an energy cascade, in which K_n again $\sim n^{-5/3}$, or an inertial subrange controlled by an enstrophy cascade. In the latter case the rate of enstrophy flow, $\frac{dP}{dt} = \gamma$ will control the spectrum.

Since $\gamma = \frac{dP}{dt}$ has units T^{-3} , dimensional arguments now require

$$K_n = f(\gamma, n) = \beta \gamma^i n^k;$$

$$\therefore L^3T^{-2} = T^{-3i} L^{-k}; \quad i = \frac{2}{3}, \quad k = -3,$$

$$K_n = \beta \gamma^{2/3} n^{-3}$$

Experiments indicate that, when there is a 2D inertial subrange, energy cascades upscale and enstrophy downscale, simultaneously, in different parts of the wave number spectrum.

Chamey showed that Q-G turbulence was like 2D turbulence¹. This seems to explain Winn-Nielsen's result.

The above average result obscures a lot of interesting behaviors – e.g., how does K_n differ between winter and summer, and between SEs and TEs? If we break up the wind fields in our conventional manner:

$$\mathbf{u} = \bar{\mathbf{u}} + \mathbf{u}' = [\bar{\mathbf{u}}] + \bar{\mathbf{u}}^* + \mathbf{u}',$$

$$K = \frac{1}{2}(\mathbf{u}^2 + \mathbf{v}^2):$$

$$\therefore [\bar{K}] = \frac{1}{2}[\bar{\mathbf{u}}^2 + \bar{\mathbf{v}}^2] = \frac{1}{2}[\bar{\mathbf{u}}^2 + \cancel{2\bar{\mathbf{u}}\bar{\mathbf{u}}'} + \bar{\mathbf{u}}'^2 + \bar{\mathbf{v}}^2 + \cancel{2\bar{\mathbf{v}}\bar{\mathbf{v}}'} + \bar{\mathbf{v}}'^2]$$

$$= \frac{1}{2}[\bar{\mathbf{u}}^2 + \cancel{2[\bar{\mathbf{u}}]\bar{\mathbf{u}}'^*} + \bar{\mathbf{u}}'^{*2} + \bar{\mathbf{v}}^2 + \cancel{2[\bar{\mathbf{v}}]\bar{\mathbf{v}}'^*} + \bar{\mathbf{v}}'^{*2}] + \frac{1}{2}[\bar{\mathbf{u}}'^2 + \bar{\mathbf{v}}'^2]$$

$$\therefore [\bar{K}] = \frac{1}{2}\{[\bar{\mathbf{u}}]^2 + [\bar{\mathbf{v}}]^2\} + \frac{1}{2}[\bar{\mathbf{u}}'^{*2} + \bar{\mathbf{v}}'^{*2}] + \frac{1}{2}[\bar{\mathbf{u}}'^{-2} + \bar{\mathbf{v}}'^{-2}]$$

$$= \bar{K}_{\text{mean}} + \bar{K}(\text{S.E.}) + \bar{K}(\text{T.E.}) = \bar{K}_0 + \sum_{n=1}^{\infty} \bar{K}_n;$$

$$\therefore \bar{K}_0 = \frac{1}{2}\left\{\tilde{\mathbf{u}}(0)^2 + \tilde{\mathbf{v}}(0)^2 + \overline{\tilde{\mathbf{u}}'(0)^2} + \overline{\tilde{\mathbf{v}}'(0)^2}\right\},$$

$$\bar{K}_n(\text{S.E.}) = \overline{\tilde{\mathbf{u}}^*(n)\tilde{\mathbf{u}}^*(-n)} + \overline{\tilde{\mathbf{v}}^*(n)\tilde{\mathbf{v}}^*(-n)} \text{ and}$$

$$\bar{K}_n(\text{T.E.}) = \overline{\tilde{\mathbf{u}}'(n)\tilde{\mathbf{u}}'(-n)} + \overline{\tilde{\mathbf{v}}'(n)\tilde{\mathbf{v}}'(-n)}, \text{ where here we have used * to indicate the SE component. Note that } \bar{K}_0 \text{ contains a contribution from time variations.}$$

Julian et al (1970) have computed $\bar{K}_n(\text{T.E.})$ for various latitudes and pressure levels.

They used NMC's analyses for the wind fields. To get a winter spectrum, they used data for every fifth day during January and February, for 6 years (1963-1968). The results for 500mb at 50N are shown on the next page (see Fig. 1 and 2 in Julian et al (1970)). 50N is the latitude where $K(\text{T.E.})$ peaks, and \therefore this result should be characteristic of T.E.'s.

The winter spectrum is very similar to Win-Nielsen's—very flat at low wave-numbers (the peak is actually at $n = 3$) and very steep at large wave numbers, with slope close to -3. The results are similar at different pressure levels and different latitudes (in mid-latitudes). To get a summer spectrum, they used NMC data for every 5th day during July and August for 5 years (1963-1967). The results for 500mb, 50N are shown in Figure 2 of Julian et al. (1970). We see a very interesting difference in summer. Now there is a pronounced peak at $n = 6$, with the spectrum falling off at low wave numbers to $\sim 1/2$ as

¹ But see Tang & Welch, 2001, *JAS*, 58, 2009. One must assume that the troposphere is bounded above – presumably the tropopause acts like a lid.

much kinetic energy. At high wave numbers, the spectrum still falls off sharply with slope $\cong -3$. Again, the results are not sensitive to latitude or level. The seasonal change in the total hemispheric kinetic energy in TE calculated by Peixoto and Oort (1974) from the 1st 5 years in the MIT general circulation library is shown in their Figure 1.

If we put these results together, we get the relative changes in kinetic energy shown in the table below:

	$1 \leq n \leq 6$	$7 \leq n \leq 18$	Total
Summer	0.57	0.40	0.97
Winter	1.40	0.60	2.00

Thus the main seasonal change in TE's is a large increase in the long-wave component in winter which eliminates the peak at $n = 6$. Thus one must distinguish at least two different kinds of TE's as being important: synoptic scale TE's, which are always present and show rather little seasonal change; and planetary scale TE's, which are primarily a winter phenomenon.

Julian et al also calculated a low latitude spectrum, from NMC data for every day during March – August, 1968, for 10N, 200mb. The result is shown in their Figure 7. Because of the greater circumference of the earth in low latitudes they could resolve higher wave numbers. The low-wave part of the spectrum contrasts strongly with mid-latitudes: it peaks at $n = 1$ and falls off monotonically for higher n . The slope of the curve for large n is somewhat less steep than in mid-latitudes, more like -2.5 than -3. This is the only low latitude spectrum that has been published.

\bar{K}_n (S.E.) has been calculated by Holopainen (1970) from 40 year mean monthly maps of pressure-surface heights (presumably by calculating geostrophic winds from them). He averaged \bar{K}_n over 15N – 90N latitudes and 100 – 1000mb pressures, and calculated it for summer and winter (although he did not say which or how many months he included in his definitions of these seasons). The results are shown (now on a linear scale) in Fig. 3 of Holopainen, (1970). There is a sharp contrast with the TE's: a strong peak at $n = 1$ in both seasons (about 50% of the total energy in $1 \leq n \leq 6$) and very little energy for $n \geq 5$. The main seasonal change is caused by the prominence of the Aleutian and Icelandic lows in winter, which are $\sim 120^\circ$ of longitude apart. The seasonal change in the total \bar{K} (S.E.), calculated by Peixoto and Oort (1974) is very similar to the seasonal change in \bar{K} (T.E.). In most months \bar{K} (SE) $\cong 25\%$ of \bar{K} (TE). The only notable exception is in April and May when the ratio is 13%.

Heat Flux Correlations:

Eddy meridional sensible heat transports depend on the correlations between v and T . If the correlations are high, the transport is very efficient, and if they are low, it is inefficient. In the case of stationary eddies, whose amplitudes peak near 50N, we can

calculate the mean correlations using the following vertical mean statistics from Oort (1971, NOAA Professoral Paper #5). We find:

$$\text{January: } [\overline{v^*T^*}] = 12.3(\text{m/s})\text{K}, [\overline{T^{*2}}] = 27.3\text{K}^2, [\overline{v^{*2}}] = 25\text{m}^2/\text{s}^2,$$

$$\therefore \text{correlation} = \frac{12.3}{5.22 \times 5} = 0.47$$

$$\text{July: } [\overline{v^*T^*}] = -0.8(\text{m/s})\text{K}, [\overline{T^{*2}}] = 5.1\text{K}^2, [\overline{v^{*2}}] = 4\text{m}^2/\text{s}^2$$

$$\therefore \text{correlation} = \frac{-0.8}{2.26 \times 2} = -0.18$$

These correlations are consistent with the sensible heat transports which we looked at earlier: $[\overline{v^*T^*}]$ is very strong in winter when the SEs are very efficient at transporting heat, but disappears in summer, when the correlation is actually negative. Thus SE's are fundamentally different in winter and summer. These results are also relevant for the eddies' energy cycle (see section 8 of this course.). The energy sources for SE's are shown by Holopainen's analysis of their energy cycle (see Fig. 1 in Holopainen (1970)). In summer their energy source is generation of eddy available potential energy by diabatic heating, but in winter their source is mean available potential energy (see section 8). Thus stationary eddies are fundamentally different in winter and summer.

In similar fashion we can calculate the correlations associated with the transient eddy meridional sensible heat fluxes, again using Oort's (1971, NPP #5) data. Using vertical means at the latitudes where $[\overline{v'T'}]$ peaks (60N in January and 55N in July), we have:

$$\text{January: } [\overline{v'T'}] = 8.6(\text{m/s})\text{K}, [\overline{v'^2}] = 126(\text{m}^2/\text{s}^2), [\overline{T'^2}] = 35.3\text{K}^2$$

$$\therefore \text{correlation} = \frac{8.6}{11.2 \times 5.94} = 0.13$$

$$\text{July: } [\overline{v'T'}] = 5.4(\text{m/s})\text{K}, [\overline{v'^2}] = 85\text{m}^2/\text{s}^2, [\overline{T'^2}] = 16.1\text{K}^2.$$

$$\therefore \text{correlation} = \frac{5.4}{9.75 \times 4.01} = 0.14$$

Thus the efficiency of the transient eddy flux is rather low, and is about the same in both reasons. Note in particular that the transient eddies are much less efficient at transporting sensible heat than are the stationary eddies in winter.

Spectra of Eddy Sensible Heat Flux: Solomon (1993)² has used 10 (9) years of ECMWF analyses to calculate the spectra (zonal wave number) of eddy sensible heat fluxes. Figure 1 in Solomon (1993) (shown below) shows the results for 51N, 850mb (the latitude and level of the peak) in January for the TE and total eddy sensible heat flux. We note that the peaks occur at $n = 5$ for TE's and $n = 2$ for SE's, i.e., the heat transporting transient eddies are very large, $\sim 5000\text{km}$ wavelength. These are not the small scale intense cyclones. Figures 4.12 and 4.13 in Solomon (1995) (also shown below) show the seasonal changes. As we noted earlier, the TE changes are relatively small. Only in summer is there a substantial decrease. The TE's peak at $n = 5$ or 6 in all seasons; the SE's at $n = 2$. Note that SE wave numbers 1 & 2 have negative transports in summer, consistent with Oort & Peixoto's result that P_M is not an energy source for SE's in summer (see section 8).

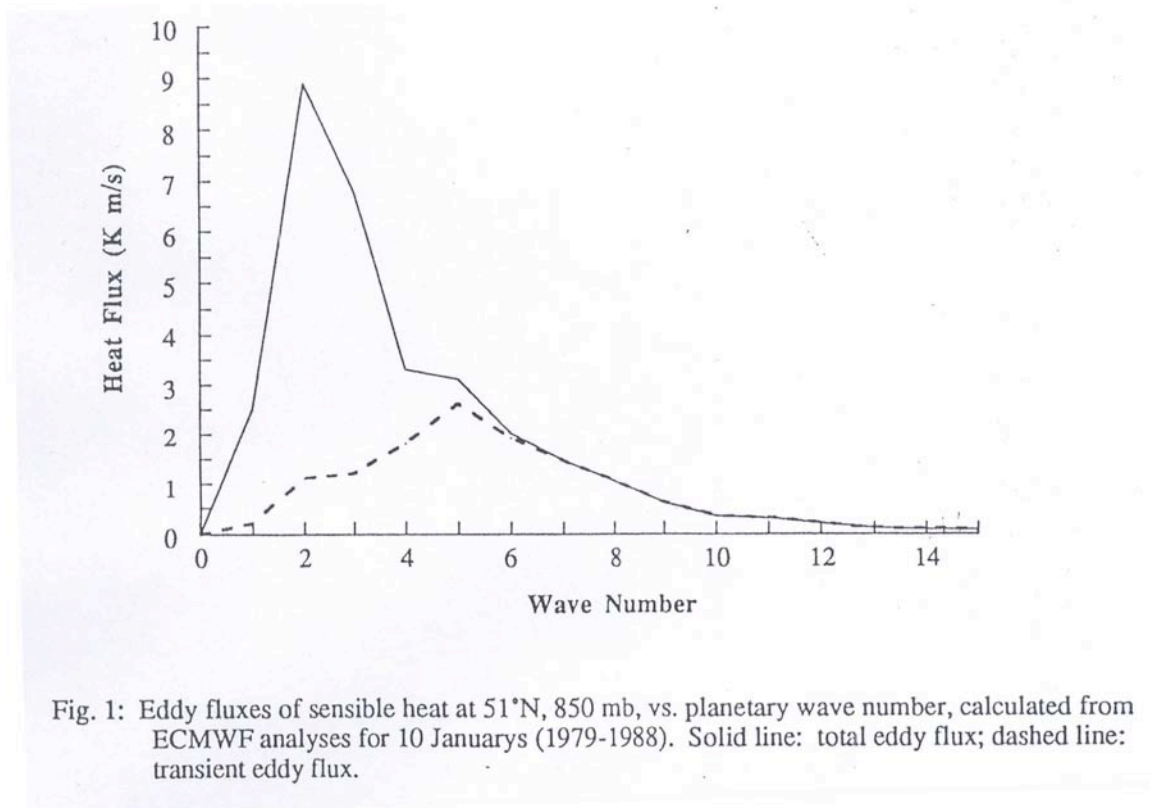


Fig. 1: Eddy fluxes of sensible heat at 51°N, 850 mb, vs. planetary wave number, calculated from ECMWF analyses for 10 Januarys (1979-1988). Solid line: total eddy flux; dashed line: transient eddy flux.

From Solomon (1993). Used with permission.

² Only the TE spectra are included in her published 1997 paper. Her earlier results are from her 1993 term paper in this course.

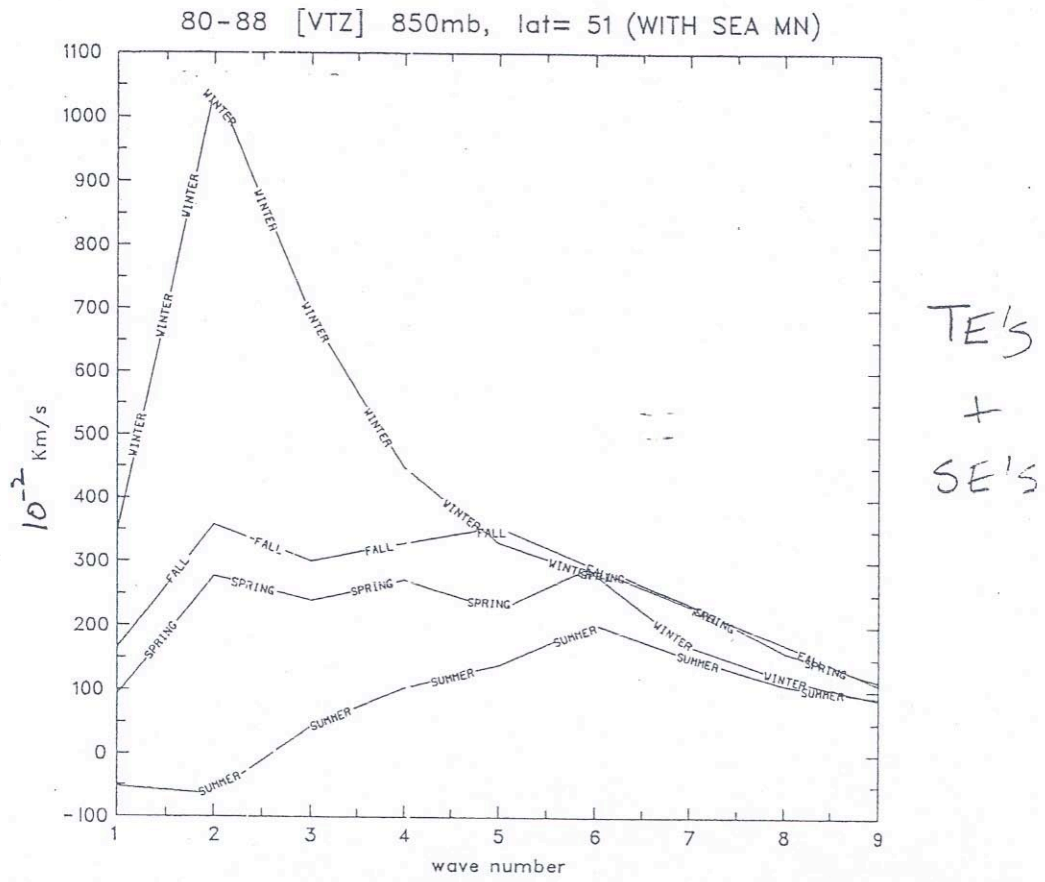
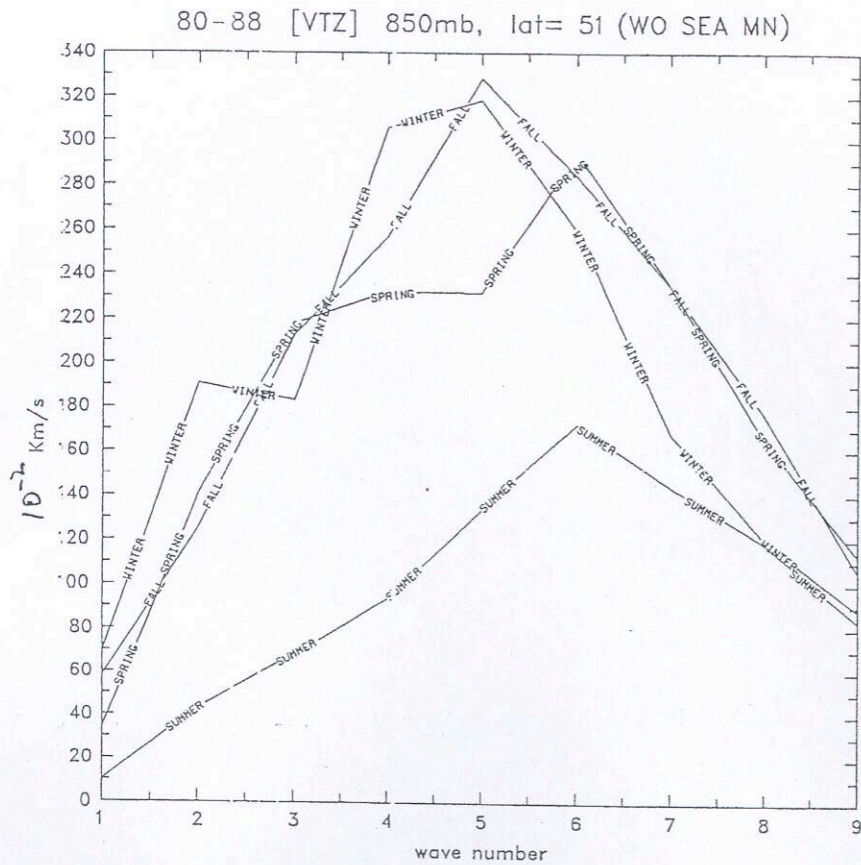


Figure 4.12: 80-88 zonal mean eddy heat flux, at 850 mb and 51N, as a function of zonal wavenumber.

From Solomon (1995). Used with permission.



TE'S
only

Figure 4.13: 80-88 zonal mean eddy heat flux, at 850 mb and 51N, with the seasonal mean removed, as a function of zonal wavenumber. (SES)

After Solomon (1997). Used with permission.

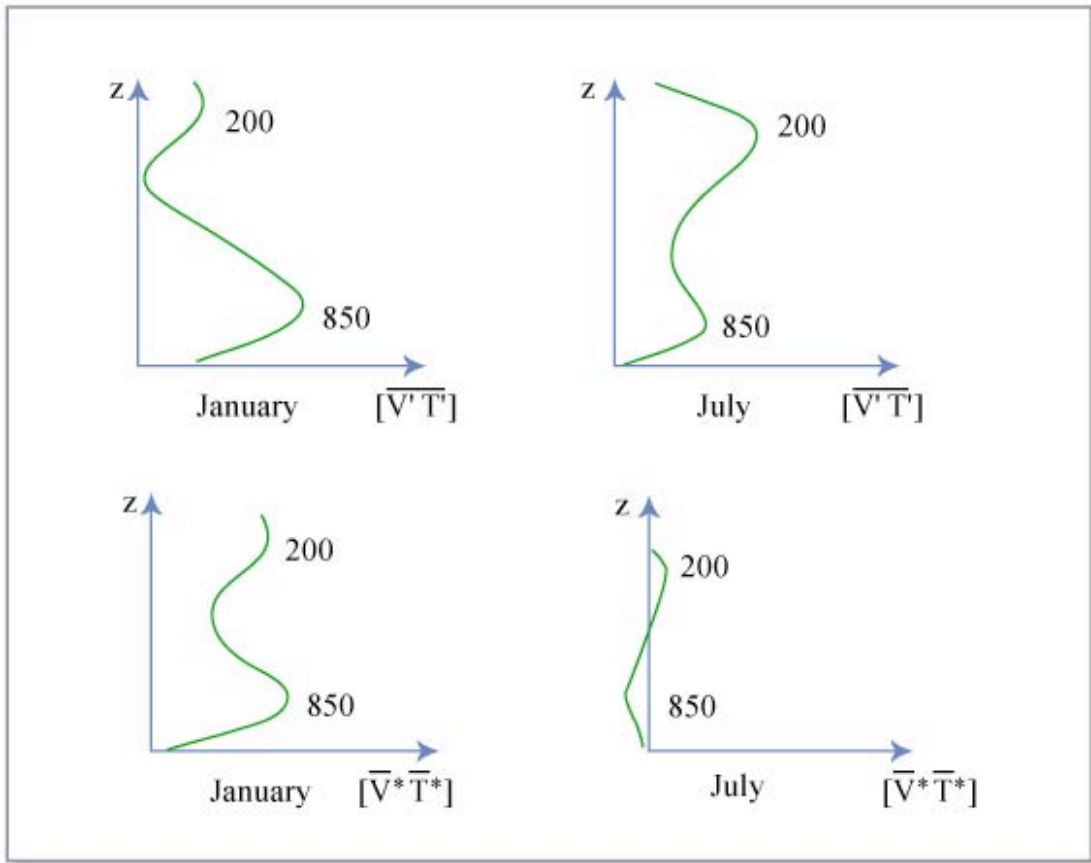


Figure by MIT OCW.

The vertical distribution of eddy transports (see schematic above) actually shows two peaks: at 850 and 200 mb. TE's in winter have the larger peak at 850 mb, but in summer at 200 mb. SE's in winter have comparable peaks at both. Thus we need to look at spectra at 200 mb, as well (see Figures 4.20 and 4.21 in Solomon (1995) also shown below). The TE's at 200 mb peak at $n = 5$ or 6 in fall or summer, as at 850 mb, but they peak at $n = 3$ in spring & winter, i.e., in those latter seasons the longer TE's have greater vertical extent. In winter the SE's peak at $n = 1$ and 3 at 200 mb, instead of $n = 2$, i.e., again these different wave numbers must have different attenuation properties.

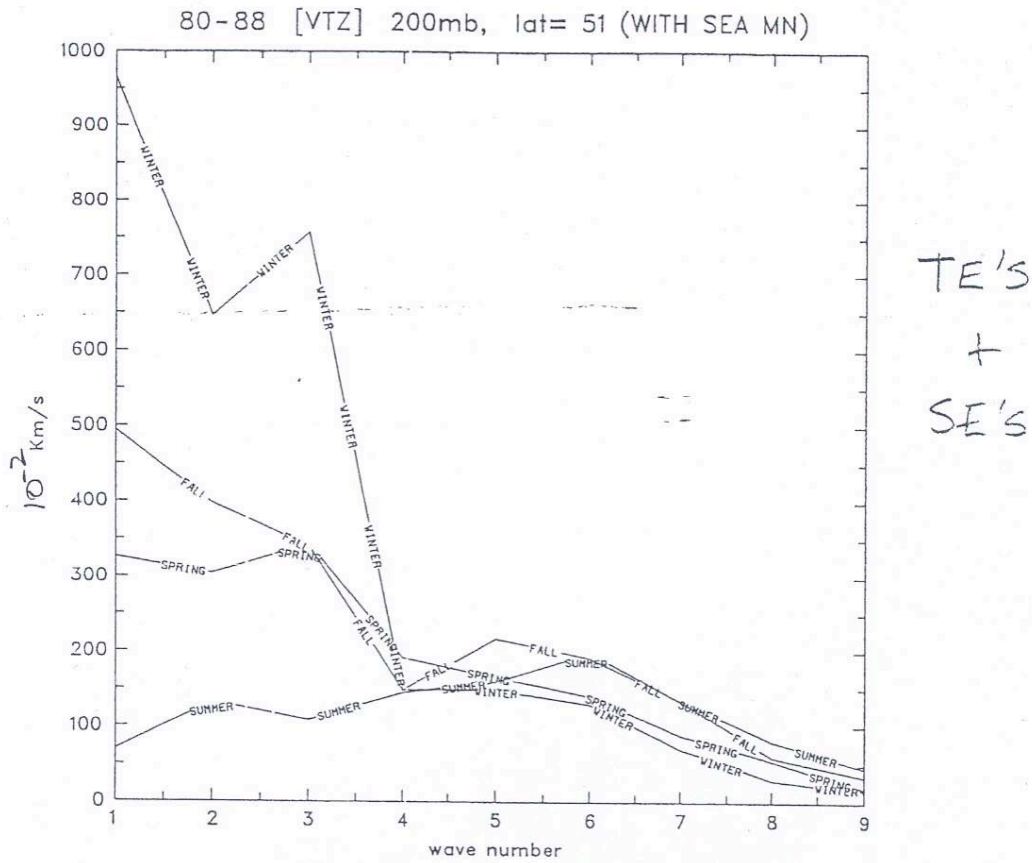


Figure 4.20: 80-88 zonal mean eddy heat flux, at 200 mb and 51N, as a function of zonal wavenumber.

From Solomon (1995). Used with permission.

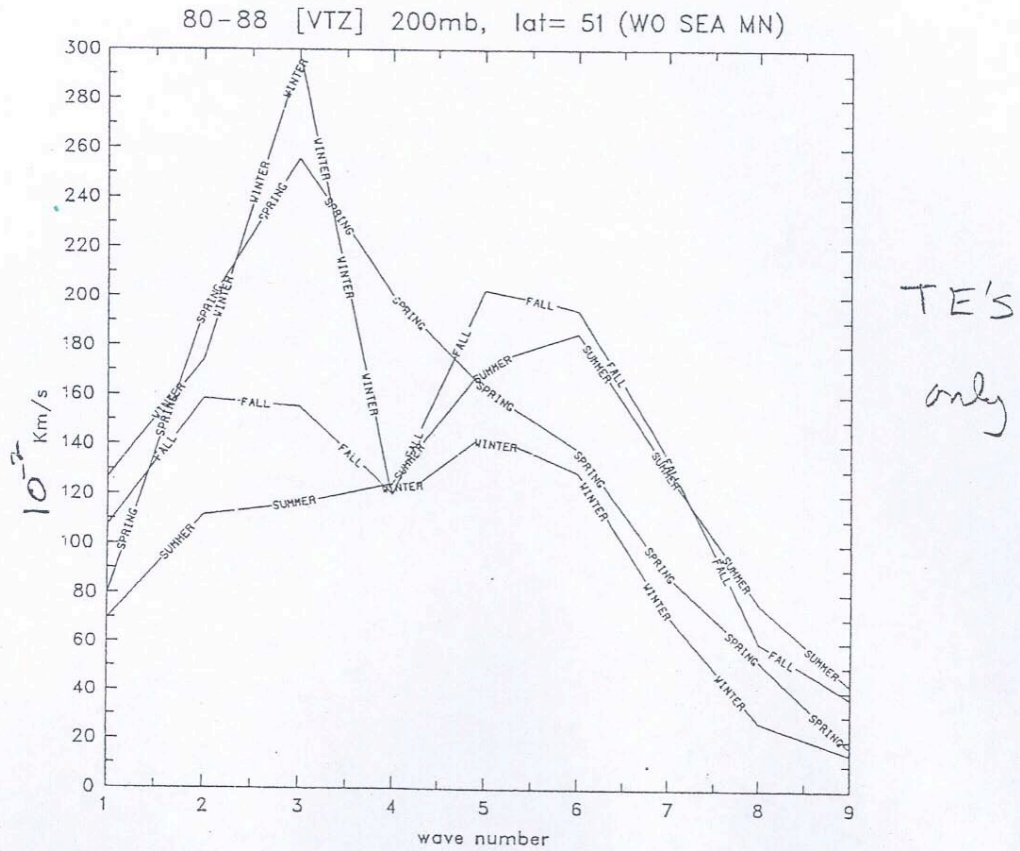


Figure 4.21: 80-88 zonal mean eddy heat flux, at 200 mb and 51N , with the seasonal mean removed, as a function of zonal wavenumber.

After Solomon (1997). Used with permission.

Figures 4.1 and 4.7 in Solomon (1993) (shown below) shows results for the Southern Hemisphere at 850 and 200 mb. There are no appreciable SE's, so these statistics all apply to TE's. At 850 mb, like the Northern Hemisphere, the peaks are at $n = 4$ to 6 in all seasons, with a slight tendency towards higher wave numbers in summer. At 200 mb, again like the Northern Hemisphere, the peak in summer and fall is at $n = 5$ or 6 , but in winter and spring it shifts to $n = 2$ or 3 . Also at either level, the seasonal change is comparable to that for TE's in the Northern Hemisphere, but much less than that for SE's.

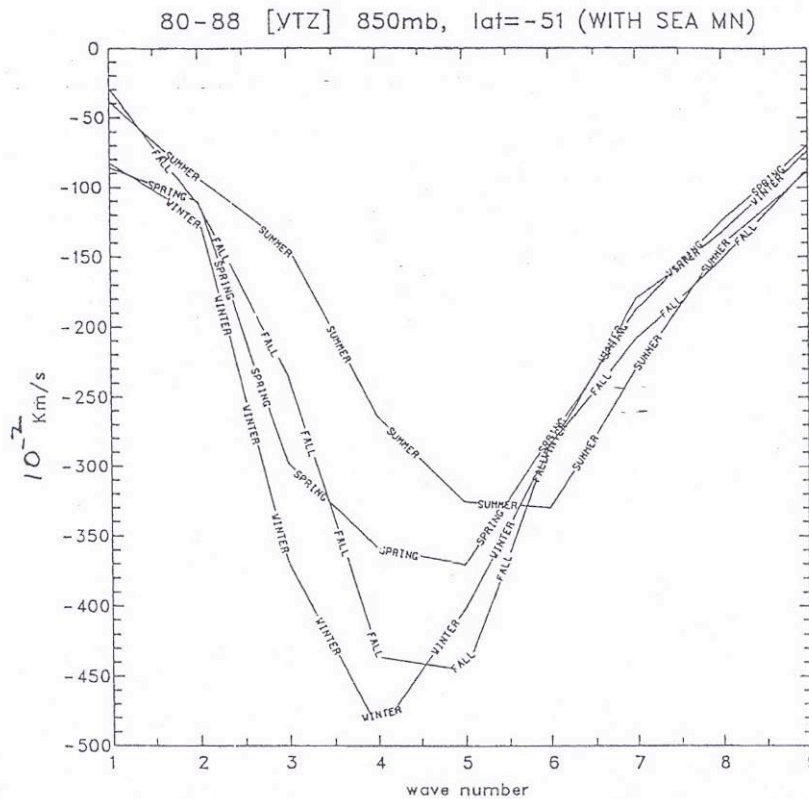


Figure 4.1: 80-88 zonal mean eddy heat flux, at 850 mb and 51S, as a function of zonal wavenumber.

From Solomon (1995). Used with permission.

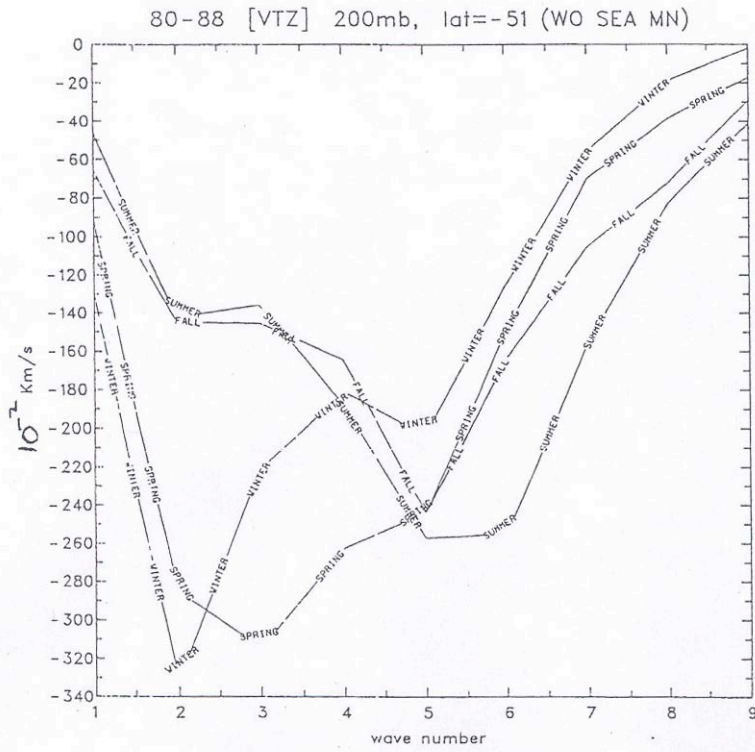


Figure 4.7: 80-88 zonal mean eddy heat flux at 200 mb and 51S, with the seasonal mean removed, as a function of zonal wavenumber.

After Solomon (1997). Used with permission.